Dalton Transactions

Accepted Manuscript

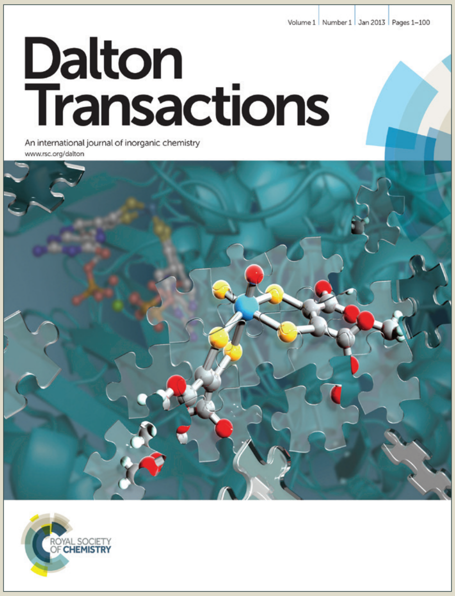

ROYAL SOCIETY OF CHEMISTRY

www.rsc.org/dalton

Synthesis and Structures of Doubly-Bridged Dicyclopentadienyl Dinuclear Rhenium Complexes, and Their Photochemical Reactions with Aromatic Halides in Benzene†

Bolin Zhu,* Xinwei Huang and Xiaoting Hao

Reaction of the doubly-bridged biscyclopentadienes ($(C_5H_4(EMe_2))(C_5H_4(SiMe_2))$) (E = Si(**1a**), or C(**1b**)) with $Re_2(CO)_{10}$ in refluxing mesitylene gave the corresponding dirhenium carbonyl complexes $[(\eta^5\text{-}C_5H_3)_2(EMe_2)(SiMe_2)][Re(CO)_3]_2$ (*trans*-**2a**,**b** and *cis*-**2a**,**b**), and the desilylated products $[(\eta^5\text{-}C_5H_4)_2(EMe_2)][Re(CO)_3]_2$ (**3a**,**b**). Photolysis of *trans*-**2a**,**b** with a series of aryl halides in benzene results in the formation of biphenyl, together with the corresponding rhenium dihalide complexes *trans*-$[(\eta^5\text{-}C_5H_3)_2(EMe_2)(SiMe_2)][Re(CO)_3][Re(CO)_2X_2]$ (X = Cl, Br, I) (**4**, **6**, **8**, or **10**) and *trans*-$[(\eta^5\text{-}C_5H_3)_2(EMe_2)(SiMe_2)][Re(CO)_2X_2]_2$ (**5**, **7**, or **9**). Additional experiments indicate that one phenyl ring in the resulting biphenyl comes from aryl halides and the other phenyl ring comes from solvent benzene. However, photolysis of *trans*-**2a** with benzyl chloride and *n*-hexyl chloride in benzene afforded the corresponding bibenzyl and *n*-dodecane, as well as the rhenium dichlorides **8** and **9**. In addition, complex *trans*-**2a** can also activate C–F bond on C_6F_6 to form the pentafluorophenyl rhenium fluoride *trans*-$[(\eta^5\text{-}C_5H_3)_2(SiMe_2)_2][Re(CO)_3][Re(CO)_2(C_6F_5)F]$ (**11**). Molecular structures of *cis*-**2a**, *cis*-**2b**, *trans*-**2b**, **3b**, **6**, **7**, **8**, **11**, and **12** determined by X-ray diffraction are also presented.

Tianjin Key Laboratory of Structure and Performance for Functional Molecules; Key Laboratory of Inorganic-Organic Hybrid Functional Material Chemistry, Ministry of Education; College of Chemistry, Tianjin Normal University, Tianjin 300387, People's Republic of China. E-mail: hxxyzbl@gmail.com; Fax: (8622)23766532; Tel: (8622)23766515

† Electronic supplementary information (ESI) available: CCDC reference numbers 1017441–1017449. For ESI and crystallographic data in CIF or other electronic format see DOI:

Introduction

The chemistry of cyclopentadienylrheniumtricarbonyl complexes (η^5-C_5R_5)Re(CO)$_3$ (R = H, Cp or Me, Cp*) has been investigated widely in recent decades, especially serving as useful precursors to produce complexes of the type (η^5-C_5R_5)Re(CO)$_2$L when they are irradiated in the presence of PR_3,[1] alkene,[2] or THF.[5] Besides, (η^5-C_5R_5)Re(CO)$_3$ could also be used in the catalytic borylation of alkanes,[4] activation of C–H bond in alkanes[5] or cycloalkanes,[6] activation of Si–H bond in silanes,[7] and H–H bond in H_2,[8] activation of C–H,[9] C–F,[10] or C–Cl[11] bond in aryl halides and allyl halides. Recently, we studied the photochemical reactions of (η^5-C_5R_5)Re(CO)$_3$ with aryl halides in benzene, and observed the stoichiometric formation of biphenyl, as well as the corresponding rhenium dicarbonyl products (η^5-C_5R_5)Re(CO)$_2$X$_2$ (X = Cl, Br, or H).[12] Bridged dicyclopentadienyl dirhenium analogues, as the bridged ligand binds two reactive metal centers, may promote the unique chemical reactivity and catalytic properties, however, their chemistry on either reactivity or application has been rarely reported. To the best of our knowledge, only a few examples of synthesis and structures have been reported.[13] Herein, in this paper we report our findings on synthesis and structures of a group of doubly-bridged dicyclopentadienyl dirhenium complexes, and their photochemical reactions with a series of aryl halides in benzene.

Results and Discussion

Synthesis of doubly-bridged dicyclopentadienyl dirhenium carbonyl complexes

Thermal treatment of the doubly-bridged biscyclopentadienes $(C_5H_4(EMe_2))(C_5H_4(SiMe_2))$ (E = Si(**1a**), or C(**1b**)) with $Re_2(CO)_{10}$ in refluxing mesitylene to give the corresponding dirhenium carbonyl complexes $[(\eta^5\text{-}C_5H_3)_2(EMe_2)(SiMe_2)][Re(CO)_3]_2$ (*trans*-**2a**,**b** and *cis*-**2a**,**b**), and the desilylated products $[(\eta^5\text{-}C_5H_4)_2(EMe_2)][Re(CO)_3]_2$ (**3a**,**b**) (Scheme 1). Comparing with *cis* isomers *cis*-**2a**,**b**, *trans* isomers *trans*-**2a**,**b** are the major products. All products were fully characterized by NMR, IR, and EA. Besides, the structures of *cis*-**2a**, *trans*-**2b**, *cis*-**2b**, and **3b** were confirmed by the single-crystal X-ray diffraction (*vide infra*).

Scheme 1. Reactions of the doubly-bridged dicyclopentadienes (**1a**,**b**) with $Re_2(CO)_{10}$.

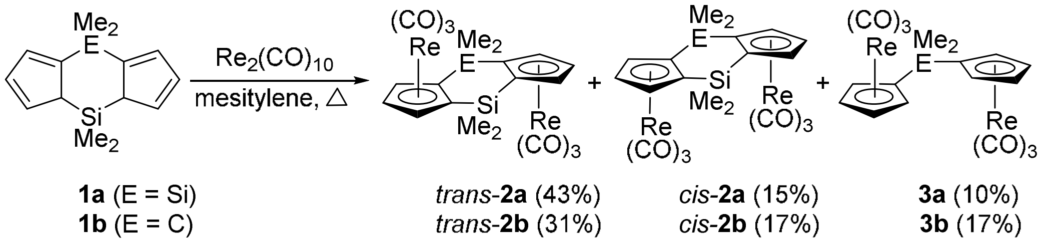

Crystal structures of *cis*-2a,b, *trans*-2b, and 3b

The molecular structures of *cis*-**2a**,**b** are shown in Figures 1-2, in both of which two Re(CO)$_3$ units are located on the same site of the doubly-bridged ligands, and the Re atoms exhibit a three-legged piano-stool geometry. In *cis*-**2a**, the conformation of the $[(\eta^5\text{-}C_5H_3)_2(SiMe_2)_2]$ ligand (∠Cp–Cp fold angle 157.6°) is significantly bent, and two Re(CO)$_3$ units are coordinated to the convex surface of the doubly-bridged ligand, which is consistent with the long Re–Re nonbonding distance (5.710 Å). There is almost no twist along the Re–Re axis, as indicated by the torsion angle ∠Cp(centroid)–Re(1)--Re(2)–Cp(centroid) (0.6). In *cis*-**2b**, the conformation of the $[(\eta^5\text{-}C_5H_3)_2(CMe_2)(SiMe_2)]$ ligand (∠Cp–Cp fold angle 175.2°) is almost flat, and the Re–Re nonbonding distance is 4.896 Å, which is shorter than that in *cis*-**2a**. Two Cp rings of the bridging ligand are slightly twisted with respect to each other, which is evident in a small torsion angle ∠Cp(centroid)–Re(1)--Re(2)–Cp(centroid) (2.3°).

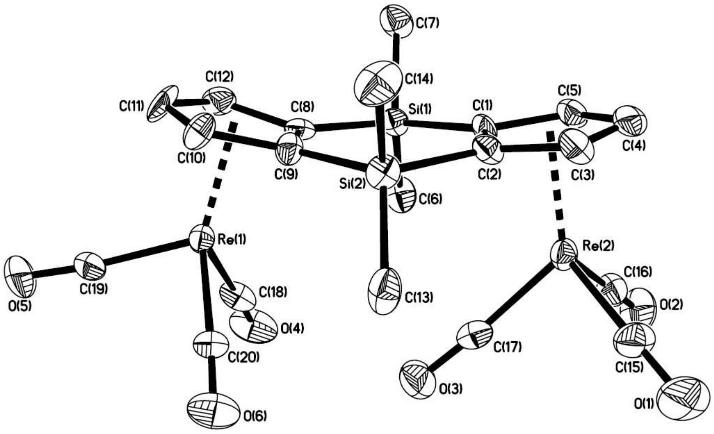

Figure 1. Thermal ellipsoid drawing of *cis*-$[(\eta^5\text{-}C_5H_3)_2(SiMe_2)_2]Re_2(CO)_6$ (*cis*-**2a**) showing the labeling scheme and 30% probability ellipsoid; hydrogens are omitted for clarity. Selected

bond lengths [Å] and angles [°] are Re(1)--Re(2) 5.710, Re(1)–C(18) 1.95(2), Re(1)–C(19) 1.89(2), Re(1)–C(20) 1.90(2), Re(1)–Cp(centroid) 1.966, Si(1)–C(1) 1.87(2), Si(1)–C(8) 1.84(2), Si(2)–C(2) 1.91(2), Si(2)–C(9) 1.87(2), Re(2)–C(15) 1.90(2), Re(2)–C(16) 1.91(3), Re(2)–C(17) 1.91(2), Re(2)–Cp(centroid) 1.984, ∠C(1)–Si(1)–C(8) 104.5(8), ∠C(6)–Si(1)–C(7) 108(1), ∠C(2)–Si(2)–C(9) 105.6(8), ∠C(13)–Si(2)–C(14) 108(1), ∠Cp(centroid)–Re(1)--Re(2)–Cp(centroid) 0.6, ∠Cp–Cp fold angle 157.6.

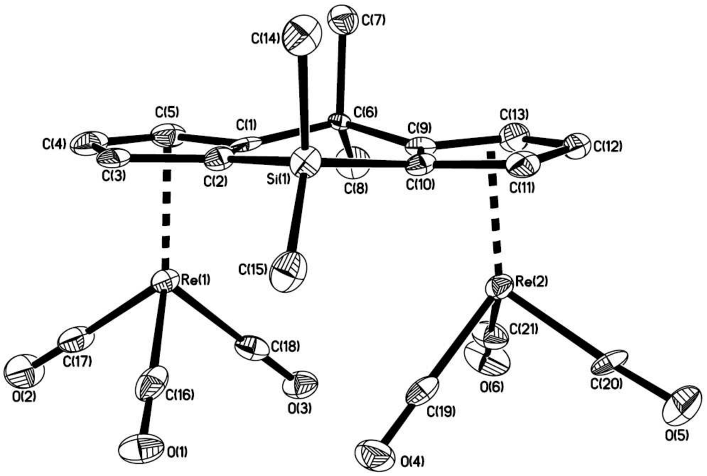

Figure 2. Thermal ellipsoid drawing of *cis*-$[(\eta^5\text{-}C_5H_3)_2(CMe_2)(SiMe_2)]Re_2(CO)_6$ (*cis*-**2b**) showing the labeling scheme and 30% probability ellipsoid; hydrogens are omitted for clarity. Selected bond lengths [Å] and angles [°] are Re(1)--Re(2) 4.896, Re(1)–C(16) 1.924(7), Re(1)–C(17) 1.932(7), Re(1)–C(18) 1.921(6), Si(1)–C(2) 1.847(6), Si(1)–C(10) 1.868(6), Re(1)–Cp(centroid) 1.975, Re(2)–Cp(centroid) 1.974, ∠C(1)–C(6)–C(9) 111.9(4), ∠C(2)–Si(1)–C(10) 99.3(3), ∠Re(1)–C(16)–O(1) 178.2(5), ∠Re(1)–C(17)–O(2) 178.6(6),

∠Re(1)–C(18)–O(3) 177.8(6), ∠Cp(centroid)–Re(1)--Re(2)–Cp(centroid) 2.3, ∠Cp–Cp fold angle 175.2.

The molecular structure of *trans*-**2b** is shown in Figure 3, in which two $Re(CO)_3$ units are located on the opposite site of the doubly-bridged $[(\eta^5\text{-}C_5H_3)_2(CMe_2)(SiMe_2)]$ ligand. The ligand conformation is significantly bent, as indicated by a smaller ∠Cp–Cp fold angle (134.9°). Two Cp rings are slightly twisted with respect to each other, which is evident in a small torsion angle ∠Re(1)–Cp(centroid)--Cp(centroid)–Re(2) (3.9°).

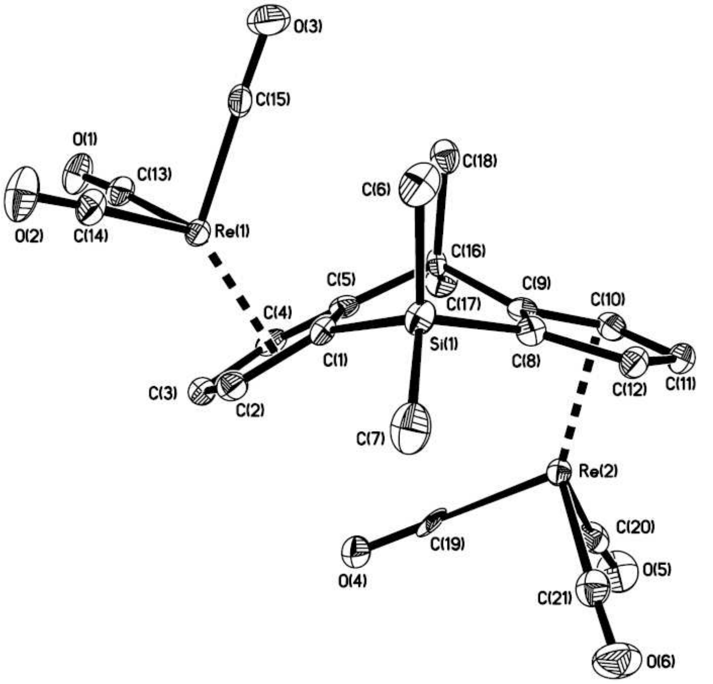

Figure 3. Thermal ellipsoid drawing of *trans*-$[(\eta^5\text{-}C_5H_3)_2(CMe_2)(SiMe_2)]Re_2(CO)_6$ (*trans*-**2b**) showing the labeling scheme and 30% probability ellipsoid; hydrogens are omitted for clarity. Selected bond lengths [Å] and angles [°] are Re(1)–C(1) 2.311(5), Re(1)–C(2) 2.271(6), Re(1)–C(3) 2.296(6), Re(1)–C(4) 2.328(5), Re(1)–C(5) 2.357(5), Re(1)–C(13) 1.910(6),

Re(1)–C(14) 1.910(6), Re(1)–C(15) 1.913(6), Si(1)–C(1) 1.862(5), Si(1)–C(8) 1.860(6), Re(1)–Cp(centroid) 1.967, Re(2)–Cp(centroid) 1.963, ∠C(5)–C(16)–C(9) 107.1(4), ∠C(17)–C(16)–C(18) 110.2(5), ∠C(1)–Si(1)–C(8) 97.4(2), ∠C(6)–Si(1)–C(7) 109.9(3), ∠Re(1)–C(13)–O(1) 175.1(5), ∠Re(1)–C(14)–O(2) 177.7(5), ∠Re(1)–C(15)–O(3) 177.8(5), ∠Re(1)–Cp(centroid)--Cp(centroid)–Re(2) 3.9, ∠Cp–Cp fold angle 134.9.

The molecular structure of **3b** is shown in Figure 4. It has an asymmetric structure. The molecule consists of two [(η^5-C_5H_4)Re(CO)$_3$] moieties liked by a CMe_2 group. The fold angle between two Cp rings is 69.7°, also there is a significant twist between them, as indicated by a torsion angle ∠Re(1)–Cp(centroid)--Cp(centroid)–Re(2) of 41.9°.

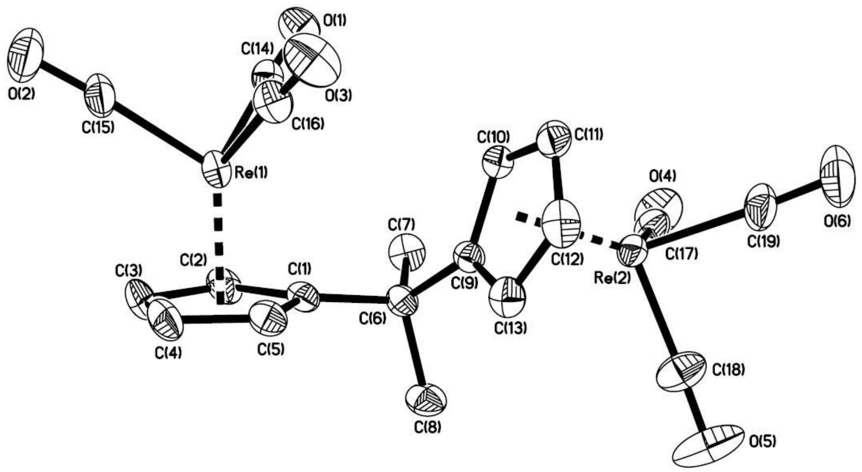

Figure 4. Thermal ellipsoid drawing of [(η^5-C_5H_4)$_2$(CMe_2)]$Re_2(CO)_6$ (**3b**) showing the labeling scheme and 30% probability ellipsoid; hydrogens are omitted for clarity. Selected bond lengths [Å] and angles [°] are Re(1)–C(1) 2.311(5), Re(1)–C(2) 2.300(5), Re(1)–C(3) 2.292(5), Re(1)–C(4) 2.291(6), Re(1)–C(5) 2.290(5), Re(1)–C(14) 1.903(5), Re(1)–C(15)

1.906(6), Re(1)–C(16) 1.912(6), Re(1)–Cp(centroid) 1.956, Re(2)–Cp(centroid) 1.953, ∠C(1)–C(6)–C(9) 108.6(4), ∠C(7)–C(6)–C(8) 108.7(4), ∠Re(1)–C(14)–O(1) 177.5(5), ∠Re(1)–C(15)–O(2) 176.0(5), ∠Re(1)–C(16)–O(3) 178.0(5), ∠Re(1)–Cp(centroid)--Cp(centroid)–Re(2) 41.9, ∠Cp–Cp fold angle 69.7.

Photochemical reactions of *trans*-2a,b with aryl halides in benzene

With complexes **2a**,**b** in hand, our initial objective was to focus on the C–X bond activation in aryl halides. The C–Br bond has the moderate activity, so the bromobenzene was used as the first substrate. Photolysis of *trans*-**2a**,**b** (λ_{max} = 365 nm) with 10 equiv of bromobenzene in benzene under N_2 for 3 h produced an orange solution. After removal of the solvent under vacuum, the residue was carefully separated in air by column chromatography on silica gel, and afforded the corresponding mono(rhenium dibromides) $[(\eta^5\text{-}C_5H_3)_2(EMe_2)(SiMe_2)][Re(CO)_3][Re(CO)_2Br_2]$ (**4**, **6**) (major products) and di(rhenium dibromides) $[(\eta^5\text{-}C_5H_3)_2(EMe_2)(SiMe_2)][Re(CO)_2Br_2]_2$ (**5**, **7**) (minor products) (Scheme 2). Interestingly, the reactions also stoichiometrically produced biphenyl (entries 1–2 in Table 1). Further activation of C–I bond and the relatively inert C–Cl bond by *trans*-**2a** was also conducted by photolysis of *trans*-**2a** with iodobenzene and chlorobenzene in benzene, which similarly provided the corresponding mono(rhenium dihalides) (**8**, **10**) and di(rhenium dichlorides) (**9**), as well as the biphenyl (Scheme 2) (entries 3–4, Table 1). These results are consistent with our recent report on the chemical reactions of $(\eta^5\text{-}C_5R_5)Re(CO)_3$ (R = Me, H) with aryl halides in benzene (entries 5–6, Table 1),[12] but different with Klahn's on the photolysis of $Cp^*Re(CO)_3$ in neat aryl chlorides, or in saturated hexane solution of aryl chlorides, which mainly yielded the corresponding insertion products Cp*Re(CO)$_2$(Ar)Cl.[11a,d] All new products (**4**-**10**) were identified by IR, NMR, and elemental analysis, in which complexes **6**, **7**, and **8** were also confirmed by the single-crystal X-ray diffraction (*vide infra*).

Scheme 2. Photolysis of *trans*-**2a**,**b** with Ph–X in Benzene.

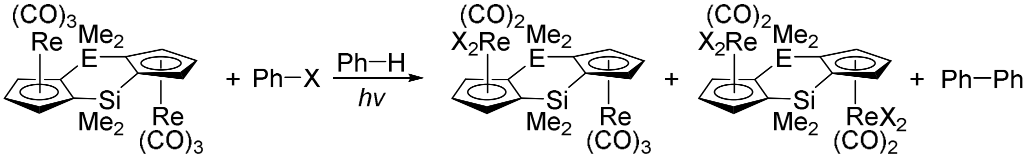

trans-**2a** (E = Si)	X = Br	**4**	**5**
trans-**2b** (E = C)	X = Br	**6**	**7**
trans-**2a** (E = Si)	X = Cl	**8**	**9**
trans-**2a** (E = Si)	X = I	**10**	

Table 1. Photolysis of Re Complexes with R–X in Benzene.[a]

$$\text{Re complexes} + \text{R–X} \xrightarrow[hv]{\text{Ph–H}} \text{R–Ph} + \text{Re products}$$

entry	R	X	Re comp.	*t* [h]	R–Ph[b]
1	Ph	Br	*trans*-**2a**	3	Biphenyl
2	Ph	Br	*trans*-**2b**	3	Biphenyl
3	Ph	I	*trans*-**2a**	9	Biphenyl
4	Ph	Cl	*trans*-**2a**	6	Biphenyl
5	Ph	Cl	$CpRe(CO)_3$	4	Biphenyl
6	Ph	Cl	$Cp^*Re(CO)_3$	2	Biphenyl
7	Ph	Cl	$Re_2(CO)_{10}$	12	–[c]
8	*p*-MeO-C_6H_4	Cl	*trans*-**2a**	4	*p*-MeO-Biphenyl
9	*p*-Me-C_6H_4	Cl	*trans*-**2a**	4	*p*-Me-Biphenyl
10	*p*-F-C_6H_4	Cl	*trans*-**2a**	4	*p*-F-Biphenyl
11	*p*-CF_3-C_6H_4	Cl	*trans*-**2a**	3	*p*-CF_3-Biphenyl
12	*p*-Cl-C_6H_4	Cl	*trans*-**2a**	2	*p*-Cl-Biphenyl
13	*m*-Cl-C_6H_4	Cl	*trans*-**2a**	2	*m*-Cl-Biphenyl
14	*o*-Cl-C_6H_4	Cl	*trans*-**2a**	6	Biphenyl *o*-Cl-Biphenyl
15[d]	Ph	Cl	*trans*-**2a**	6	*p*-Cl-Biphenyl *m*-Cl-Biphenyl
16	Bn	Cl	*trans*-**2a**	5	$PhCH_2Ph$ $PhCH_2CH_2Ph$
17	*n*-Hexyl	Cl	*trans*-**2a**	8	*n*-Dodecane
18	Cy	Cl	*trans*-**2a**	12	–[c]

[a] Reaction conditions: irradiation of Re complexes (0.05 mmol) and R–X (0.50 mmol) in 10 mL benzene solvent. [b] Biphenyl products were isolated by column chromatography, and identified by comparing their respective ^1H NMR spectra with authentic samples, the yields of biphenyl depend on the amounts of Re involved into the reaction. [c] "–" means no reaction. [d] In neat C_6H_5Cl (10 mL).

Crystal structures of 6, 7, and 8

The molecular structures of **6** and **8** are shown in Figures 5-6, which are similar to each other. Two Re units Re(CO)$_3$ and Re(CO)$_2$X$_2$ (X = Br in **6**, X = Cl in **8**) are coordinated to the respective Cp rings in η^5-mode, and located on the opposite site of the doubly-bridged ligands. The former Re atom exhibits a three-legged piano-stool geometry, and the latter shows a four-legged geometry. Besides, the two halogen atoms on the same Re center are located in *trans*-configuration. The conformation of the double-bridged ligands is significantly bent, as indicated by the respective ∠Cp–Cp fold angle (135.2° for **6**, 134.9° for **8**). Two Cp rings are slightly twisted with respect to each other, which is evident in a very small torsion angle ∠Re(1)–Cp(centroid)--Cp(centroid)–Re(2) (3.2° for **6**, 0.4° for **8**).

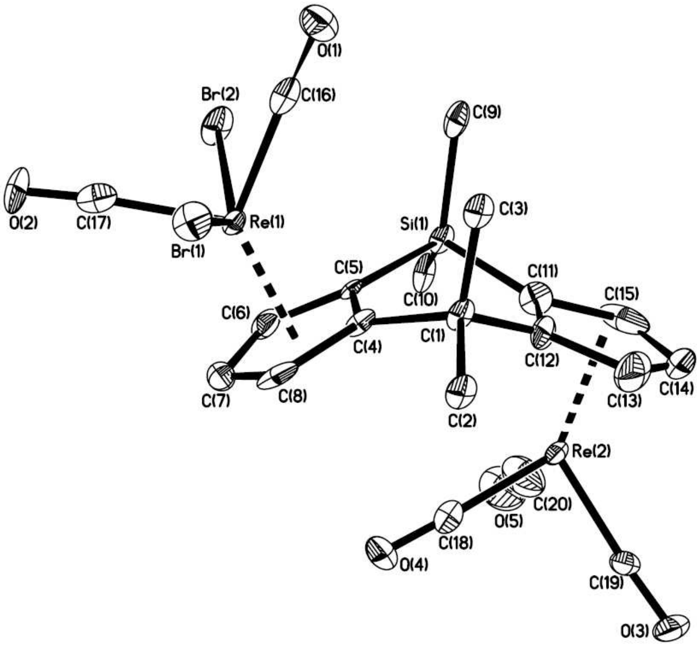

Figure 5. Thermal ellipsoid drawing of *trans*-[(η^5-C_5H_3)$_2$(CMe_2)($SiMe_2$)][$Re(CO)_3$][$Re(CO)_2Br_2$] (**6**) showing the labeling scheme and 30% probability ellipsoid; hydrogens are omitted for clarity. Selected bond lengths [Å] and angles [°] are Re(1)–Br(1) 2.5826(11), Re(1)–Br(2) 2.5956(12), Re(1)–C(16) 1.964(12), Re(1)–C(17) 1.967(12), Re(1)–Cp(centroid) 1.933, Re(2)–Cp(centroid) 1.961, ∠Re(1)–C(16)–O(1) 176.6(9), ∠Re(1)–C(17)–O(2) 174.9(10), ∠C(16)–Re(1)–Br(1) 79.0(3), ∠Br(1)–Re(1)–C(17) 79.7(3), ∠C(17)–Re(1)–Br(2) 77.6(3), ∠Br(2)–Re(1)–C(16) 75.9(3), ∠Re(1)–Cp(centroid)--Cp(centroid)–Re(2) 3.3, ∠Cp–Cp fold angle 135.2.

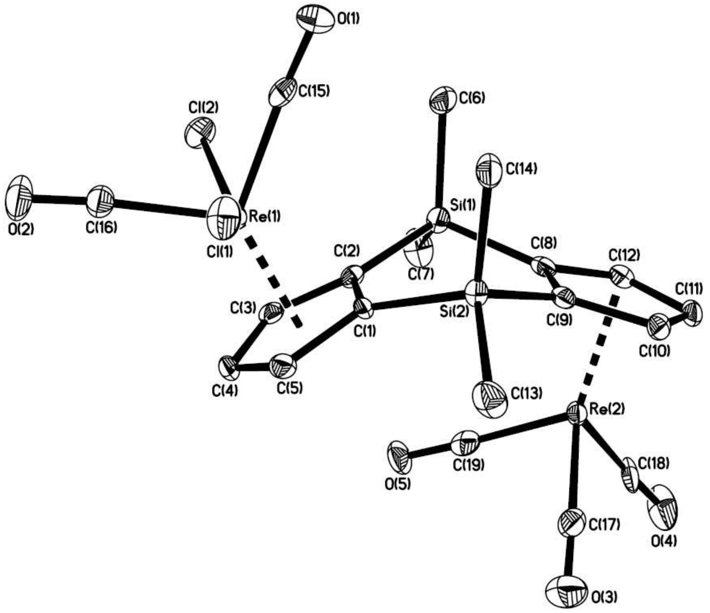

Figure 6. Thermal ellipsoid drawing of *trans*-[(η^5-C_5H_3)$_2$($SiMe_2$)$_2$][$Re(CO)_3$][$Re(CO)_2Cl_2$] (**8**) showing the labeling scheme and 30% probability ellipsoid; hydrogens are omitted for clarity. Selected bond lengths [Å] and angles [°] are Re(1)–Cl(1) 2.4467(11), Re(1)–Cl(2) 2.4462(11), Re(1)–C(15) 1.953(5), Re(1)–C(16) 1.967(5), Re(1)–Cp(centroid) 1.921,

Re(2)–Cp(centroid) 1.952, ∠Re(1)–C(15)–O(1) 176.0(4), ∠Re(1)–C(16)–O(2) 175.7(4), ∠C(15)–Re(1)–Cl(1) 77.68(13), ∠Cl(1)–Re(1)–C(16) 78.29(13), ∠C(16)–Re(1)–Cl(2) 79.92(13), ∠Cl(2)–Re(1)–C(15) 77.71(13), ∠Cp(centroid)–Re(1)--Re(2)–Cp(centroid) 0.4, ∠Cp–Cp fold angle 134.9.

The molecular structure of **7** is shown in Figures 7. Two equal Re(CO)$_2$Br$_2$ units are coordinated to the Cp rings in η^5-mode, and located on the opposite site of the doubly-bridged ligand. Again, the two bromine atoms on the same Re center are located in *trans*-configuration. The conformation of the double-bridged ligand is similarly bent to form a ∠Cp–Cp fold angle of 138.6°. Two Cp rings are slightly twisted with respect to each other, as indicated by a torsion angle ∠Cp(centroid)–Re(1)--Re(2)–Cp(centroid) (6.7°). The mean distance of Re–Br bond is 2.590 Å, and the mean distance of Re–Cp*(centroid) is 1.948 Å, which compare very well with those values (2.579(2) and 1.945(7) Å) in dibromo analogue *trans*-Cp*Re(CO)$_2$Br$_2$.[14]

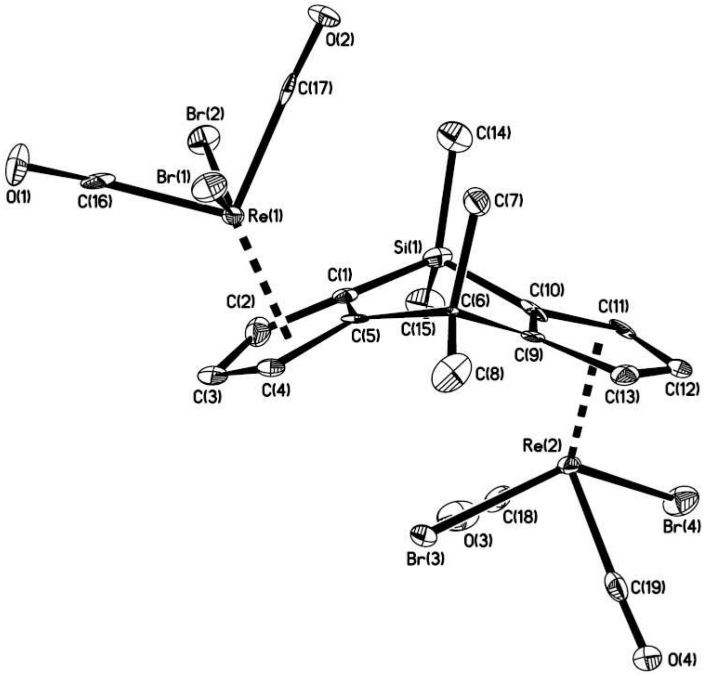

Figure 7. Thermal ellipsoid drawing of *trans*-[(η^5-C_5H_3)$_2$(CMe_2)($SiMe_2$)][Re(CO)$_2$$Br_2$]$_2$ (**7**) showing the labeling scheme and 30% probability ellipsoid; hydrogens are omitted for clarity. Selected bond lengths [Å] and angles [°] are Re(1)–Br(1) 2.5832(9), Re(1)–Br(2) 2.5864(9), Re(1)–C(16) 1.958(9), Re(1)–C(17) 1.956(9), Re(2)–Br(3) 2.5725(9), Re(2)–Br(4) 2.6176(10), Re(2)–C(18) 1.962(10), Re(2)–C(19) 1.962(9), Re(1)–Cp(centroid) 1.945, Re(2)–Cp(centroid) 1.951, ∠C(16)–Re(1)–Br(1) 77.3(2), ∠Br(1)–Re(1)–C(17) 77.6(2), ∠C(17)–Re(1)–Br(2) 77.4(2), ∠Br(2)–Re(1)–C(16) 77.8(2), ∠C(18)–Re(2)–Br(3) 77.6(3), ∠Br(3)–Re(2)–C(19) 78.1(2), ∠C(19)–Re(2)–Br(4) 78.4(2), ∠Br(4)–Re(2)–C(18) 75.4(3), ∠Cp(centroid)–Re(1)--Re(2)–Cp(centroid) 6.7, ∠Cp–Cp fold angle 138.6.

It is interesting to note that two halogen atoms on the same Re are located in *trans* position in all three complexes **6**, **7** and **8**. In general, of two isomers of rhenium dicarbonyl dihalo complex, *trans* isomer is always the main form of existence under the UV light or upon mild heating when compared with *cis* isomer.[14,15] Sutton has reported that the rhenium complexes *cis*-$Cp^*Re(CO)_2X_2$ would convert to the *trans* isomers by UV irradiation in the hexane,[15] this is consistent with the structures of products we obtained.[14]

Scope extension and mechanism discussion

Reactions listed in entries 1-6 (Table 1) show the generality of this reaction type, which generally provide biphenyl and the corresponding rhenium dihalides. However, no reaction occurred in the similar photolysis of $Re_2(CO)_{10}$ with chlorobenzene in benzene (entry 7). To expand the scope of the substrates, photolysis of various *para*-substituted chlorobenzene with *trans*-**2a** were examined, and the reactions gave similarly the rhenium chlorides **8** and **9**, and the *para*-substituted biphenyl, whether the substituent is an electron-donating (MeO, Me) or electron-withdrawing (F, CF_3, Cl) group (entries 8–12). Besides, to understand the steric effect of the reaction, photolysis of *meta*- and *ortho*-chloro substituted chlorobenzene with *trans*-**2a** were tested. For the former, the reaction afforded the expected *meta*-chloro biphenyl; for the latter (entry 13), however, the reaction formed mainly the biphenyl and only trace amount of *ortho*-chloro biphenyl (entry 14), it is possible that the vicinal substituent (Cl) affected the activation of C–Cl bond.

Next, the source of the biphenyl was investigated. Photolysis of *trans*-**2a** with 4-chloroanisole in benzene-d_6 generated the 4-methoxybiphenyl-d_5 (p-CH_3O-C_6H_4-C_6D_5), completely no biphenyl or 4,4'-dimethoxybiphenyl were observed. It is revealed that the *p*-CF_3-C_6H_4 and C_6D_5 moieties in the resulting substituted biphenyl come from 4-chlorobenzotrifluoride and solvent benzene-d_6, respectively.

For the formation of biphenyl in the photolysis of (η^5-C_5R_5)$Re(CO)_3$ (R = Mr, H) with aryl halides in benzene, we have proposed a plausible mechanism involving oxidative addition of a C–X bond on aryl halides and a C–H bond on benzene successively to Re after two CO lost, then the two Ph groups are coupled to give biphenyl by reductive elimination.[12] So we consider that the similar arguments may also be applied to the doubly-bridged dicyclopentadienyl dirhenium system (Scheme 3). First, a CO lost from Re precursor under UV irradiation to give a 16e$^-$ unsaturated species (**A**); this is followed by oxidative addition of a C–Cl bond on chlorobenzene to form **B**. In the next step, another CO lost and oxidative addition of a C–H bond on benzene from **B** results in the intermediate **C**. Then elimination of biphenyl and recoordination of CO in **C** generates the compound **D**, which is unstable when exposed to air and converts into the final Re dichloride products.[16]

Scheme 3. Proposed mechanism for photolysis of *trans*-**2a**,**b** with chlorobenzene in Benzene.

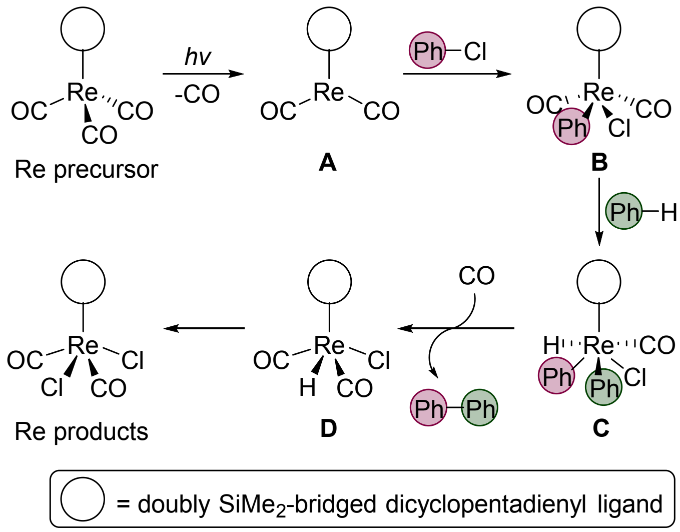

Halogen–hydrogen exchange reaction is a usual method to trap these unstable rhenium hydrides.[10] To confirm the formation of the hydride chloride complexes $[(\eta^5\text{-}C_5H_3)_2(SiMe_2)_2][Re(CO)_3][Re(CO)_2Cl(H)]$ or $[(\eta^5\text{-}C_5H_3)_2(SiMe_2)_2][Re(CO)_2Cl(H)]_2$ (Type **D** compound in Scheme 3) during the photolysis of *trans*-**2a** with chlorobenzene in benzene, excess $CHBr_3$ was added into the mixture at the end of the reaction. By routine column chromatography, the expected Br/H exchanged product $[(\eta^5\text{-}C_5H_3)_2(SiMe_2)_2][Re(CO)_3][Re(CO)_2BrCl]$ (**11**) was successfully separated, and further confirmed by the single-crystal X-ray diffraction (Figure 8), which has a similar structure as that of complex **8**.

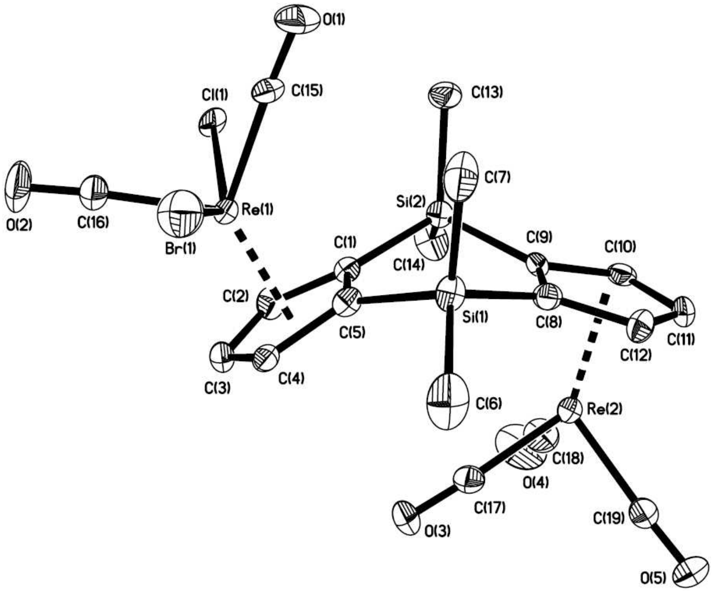

Figure 8. Thermal ellipsoid drawing of *trans*-$[(\eta^5\text{-}C_5H_3)_2(SiMe_2)_2][Re(CO)_3][Re(CO)_2BrCl]$ (**11**) showing the labeling scheme and 30% probability ellipsoid; hydrogens are omitted for

clarity. Selected bond lengths [Å] and angles [°] are Re(1)–Cl(1) 2.472(10), Re(1)–Br(1) 2.576(2), Re(1)–C(15) 1.947(9), Re(1)–C(16) 1.965(10), Re(1)–Cp(centroid) 1.926, Re(2)–Cp(centroid) 1.955, ∠Re(1)–C(15)–O(1) 176.9(9), ∠Re(1)–C(16)–O(2) 175.8(10), ∠C(15)–Re(1)–Cl(1) 75.3(16), ∠Cl(1)–Re(1)–C(16) 76.6(15), ∠C(16)–Re(1)–Br(1) 79.9(4), ∠Br(1)–Re(1)–C(15) 77.5(4), ∠Cp–Cp fold angle 135.3.

We even tried the photolysis of *trans*-**2a** in neat chlorobenzene, and obtained the mixtures of *para*-chloro biphenyl and *meta*-chloro biphenyl, together with the corresponding rhenium chlorides **8** and **9** (entry 15). It is clear that the *para* or *meta* C–H bond on chlorobenzene is activated in the second oxidative addition step. The absence of *ortho*-chloro biphenyl may suggest that the steric effect of Cl affected the activation of the *ortho* C–H bond on chlorobenzene.

Photochemical reactions of *trans*-2a with alkyl chlorides in benzene

To explore the range of application of this reaction type, several alkyl chlorides were also examined. In the photoreaction of *trans*-**2a** with benzyl chloride in benzene, the expected product diphenylmethane was obtained. Surprisingly, the reaction also afforded the other product bibenzyl (entry 16). The ratio of them is about 3:5. It is easy to understand that the former was formed according to the proposed mechanism described above (Scheme 3). The mechanism for the formation of the latter seems more straightforward. We consider that the possible mechanism could involve oxidative addition of two C–Cl bonds on benzyl chloride after two CO lost, then the two benzyl groups are coupled to give dibenzyl by reductive elimination. The reason that the Re intermediate activates the second C–Cl bond is most likely because the low C–Cl bond dissociation energy (68 kcal/mol) on benzyl chloride and the less steric effect of the benzyl group.[17] Similarly, the photoreaction of *trans*-**2a** with *n*-hexyl chloride in benzene also afforded the coupled product *n*-dodecane (entry 17). While the reaction of *trans*-**2a** with cyclohexyl chloride did not afford any products (entry 18), the possible cause is that the relatively bulky group (cyclohexyl) inhibits the activation of C–Cl bond.

Photochemical reactions of *trans*-2a in neat C_6F_6

At the end, we challenged the high energy C–F bond activation with the dirhenium complex *trans*-**2a**. The photolysis of *trans*-**2a** was performed in neat C_6F_6, which successfully produced the pentafluorophenyl rhenium fluoride *trans*-$[(\eta^5\text{-}C_5H_3)_2(SiMe_2)_2][Re(CO)_3][Re(CO)_2(C_6F_5)F]$ (**12**) by the activation of C–F bond on C_6F_6 (Scheme 5). The X-ray molecular structure of **12** is shown in Figure 9, which shows that the two carbonyls on the same Re center are located in *cis*-configuration. The similar C–F bond activation was reported by Klahn in the photolysis of $(\eta^5\text{-}C_5Me_5)Re(CO)_3$ in the presence of C_6F_6,[10] which gave the product $(\eta^6\text{-}C_5Me_4CH_2)Re(CO)_2(C_6F_5)$ via intermolecular C–F bond and intramolecular C–H bond activation. And the proposed mechanism for formation of the product involves the intermediate $(\eta^5\text{-}C_5Me_5)Re(CO)_2(\eta^2\text{-}C_6F_6)$ or the C–F bond oxidative addition intermediate $(\eta^5\text{-}C_5Me_5)Re(CO)_2(C_6F_5)F$.[18] Here we may provide an evident to support the latter intermediate.

Scheme 5. Photolysis of *trans*-2a in hexafluorobenzene.

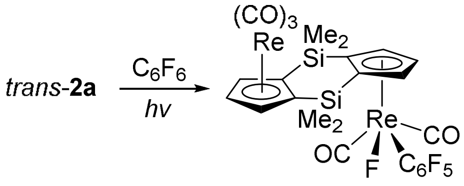

12

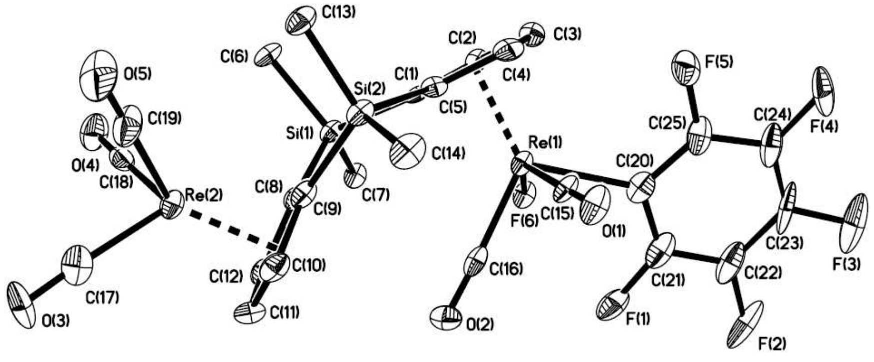

Figure 9. Thermal ellipsoid drawing of *trans*-[(η^5-C_5H_3)$_2$($SiMe_2$)$_2$][Re(CO)$_3$][Re(CO)$_2$(C_6F_5)(F)] (**12**) showing the labeling scheme and 50% probability ellipsoid; hydrogens are omitted for clarity. Selected bond lengths [Å] and angles [°] are Re(1)–F(6) 2.014(5), Re(1)–C(20) 2.194(13), Re(1)–Cp(centroid) 1.959, Re(2)–Cp(centroid) 1.969, ∠Re(1)–C(15)–O(1) 178.4(11), ∠Re(1)–C(16)–O(2) 177.4(10), ∠C(15)–Re(1)–C(20) 73.5(4), ∠C(20)–Re(1)–F(6) 77.5(4), ∠F(6)–Re(1)–C(16) 83.6(4), ∠C(16)–Re(1)–C(15) 80.0(5), ∠Cp–Cp fold angle 141.1.

Summary

In summary, we first reported synthesis and structures of a new class of doubly-bridged dicyclopentadienyl dirhenium complexes, and their photochemical reactions with aryl halides in benzene. Like their parent complex (η^5-C_5R_5)Re(CO)$_3$ (R = H or Me), the reaction general generated biphenyl and the corresponding rhenium dihalides. Additional experiments indicated that one phenyl ring in the resulting biphenyl comes from aryl halide and the other phenyl ring comes from solvent benzene. Plausible mechanism involves intermolecular C(sp^2)–X bond activation on aryl halides and C–H bond activation on solvent benzene is tentatively proposed by referring to that of similar photolysis of (η^5-C_5R_5)Re(CO)$_3$ with aryl halides. More interesting, the dirhenium complex *trans*-**2a** can activate two C(sp^3)–X bonds in alkyl chlorides (benzyl chloride and *n*-hexyl chloride) to give the corresponding coupled products (bibenzyl and *n*-dodecane), and *trans*-**2a** can also activate C–F bond on C_6F_6 to form the pentafluorophenyl rhenium fluoride. Activation of other inert bonds and the development of catalytic system with these dirhenium complexes are in progress.

Experimental

General Considerations

Schlenk and vacuum line techniques were employed for all manipulations. All solvents were distilled from appropriate drying agents under nitrogen prior to use. ^{1}H and ^{13}C NMR spectra were recorded on a Bruker AV400 instrument at room temperature. All ^{1}H NMR chemical shifts were referenced using the chemical shift of residual solvent resonance ($CDCl_3$, δ 7.26), ^{13}C NMR chemical shifts to solvent peak ($CDCl_3$, δ 77.16) and ^{19}F NMR spectrum to internal C_6F_6 at δ −162.9. IR spectra were recorded as KBr disks on a Nicolet 560 ESP FTIR spectrometer. Elemental analyses were performed on a Perkin–Elmer 240C analyzer. Photochemical reactions were carried out with a water-jacketed 500 W high-pressure Hg lamp (λ_{max} = 365 nm) as the UV source. The irradiation was conducted in a quartz tube, or in 5 mm

Pyrex NMR tubes in the ice-water bath, which was placed adjacent to the lamp. Doubly-bridged bis(cyclopentadienes) **1a–b** were prepared by the literature methods.[19]

Reaction of $(C_5H_4(SiMe_2))_2$ (1a) with $Re_2(CO)_{10}$.

A solution of $(C_5H_4(SiMe_2))_2$ (37 mg, 0.15 mmol) and $Re_2(CO)_{10}$ (100 mg, 0.15 mmol) in mestylene (5 ml) was refluxed for 40 h. After removal of the solvent under reduced pressure, the residue, which was dissolved in a minimum amount of CH_2Cl_2; the solution was chromatographed on an alumina column using petroleum ether–CH_2Cl_2 (5:1) as eluent. A colorless band was eluted and collected. Then, the second colorless band was eluted with petroleum ether–CH_2Cl_2 (3:1). Finally, another colorless band was eluted with petroleum ether–CH_2Cl_2 (1:1). After vacuum removal of the solvents from the above three eluates, the residues were recrystallized from *n*-hexane/CH_2Cl_2 (1:1) at –10 °C. From the first fraction, 50 mg (43%) of colorless crystalline *trans*-**2** was obtained. *Anal.* Calc. for $C_{20}H_{18}O_6Re_2Si_2$: C, 30.68; H, 2.32. Found: C, 30.51; H, 2.25. ^1H NMR (400 MHz, $CDCl_3$): δ_H 5.63 (d, $J = 2.4$ Hz, 4H, Cp–*H*), 5.49 (t, $J = 2.4$ Hz, 2H, Cp–*H*), 0.51 (s, 12H, Si–*Me*) ppm. ^{13}C NMR (100 MHz, $CDCl_3$): δ_c 193.8 (*C*O), 97.1, 95.1, 87.0 (Cp–*C*), 3.0 (Me–*C*) ppm. IR (KBr): [ν_{CO}/cm^{-1}] 2016 s, 1903 s. From the second fraction, 11 mg (10%) of colorless crystalline **3a** was obtained. *Anal.* Calc. for $C_{18}H_{14}O_6Re_2Si$: C, 29.75; H, 1.94. Found: C, 29.55; H, 1.83. ^1H NMR (400 MHz, $CDCl_3$): δ_H 5.46 (m, 4H, Cp–*H*), 5.44 (m, 4H, Cp–*H*), 0.46 (s, 6H, Si–*Me*) ppm.[1] IR (KBr): [ν_{CO}/cm^{-1}] 2028 s, 2018 s, 1930 s. From the third fraction, 18 mg (15%) of colorless crystalline *cis*-**2** was obtained. *Anal.* Calc. for $C_{20}H_{18}O_6Re_2Si_2$: C, 30.68; H, 2.32. Found: C, 30.18; H, 2.45. ^{1}H NMR (400 MHz, CDCl$_3$): δ_H 5.69 (t, *J* = 2.4 Hz, 2H, Cp–*H*), 5.38 (d, *J* = 2.4 Hz, 4H, Cp–*H*), 0.55 (s, 6H, Si–*Me*), 0.41 (s, 6H, Si–*Me*) ppm. IR (KBr): [ν_{CO}/cm^{-1}] 2013 s, 1940 s, 1916 s, 1904 s.

Reaction of (C_5H_4(CMe_2))(C_5H_4($SiMe_2$)) (1b) with $Re_2(CO)_{10}$.

A solution of (C_5H_4(CMe_2))(C_5H_4($SiMe_2$)) (35 mg, 0.15 mmol) and $Re_2(CO)_{10}$ (100 mg, 0.15 mmol) in mestylene (5 ml) was refluxed for 40 h, using the same method as in the reaction of **1** with $Re_2(CO)_{10}$. From the first fraction, 36 mg (31%) of colorless crystalline *trans*-**2** was obtained. *Anal.* Calc. for $C_{21}H_{18}O_6Re_2Si$: C, 32.89; H, 2.37. Found: C, 33.11; H, 2.46. ^{1}H NMR (400 MHz, CDCl$_3$): δ_H 5.56 (m, 2H, Cp–H), 5.40 (m, 2H, Cp–H), 5.26 (m, 2H, Cp–H), 1.59 (s, 6H, C–Me), 0.57 (s, 6H, Si–Me) ppm. IR (KBr): [ν_{CO}/cm^{-1}] 2018 s, 1923 s, 1901 s. From the second fraction, 18 mg (17%) of colorless crystalline **3b** was obtained. *Anal*. Calc. for $C_{19}H_{14}O_6Re_2$: C, 32.11; H, 1.99. Found: C, 32.53; H, 1.72. ^{1}H NMR (400 MHz, CDCl$_3$): δ_H 5.41 (m, 4H, C_5H_3), 5.24 (s, 4H, C_5H_3), 1.49 (s, 6H, C(CH_3)) ppm. IR (KBr): [ν_{CO}/cm^{-1}] 2024 s, 2018 s, 1950 s, 1922 s, 1887 s. From the third fraction, 20 mg (17%) of colorless crystalline *cis*-**2** was obtained. *Anal*. Calc. for $C_{21}H_{18}O_6Re_2Si$: C, 32.89; H, 2.37. Found: C, 33.11; H, 2.46. ^{1}H NMR (400 MHz, CDCl$_3$): δ_H 5.50 (m, 2H, Cp–H), 5.35 (m, 2H, Cp–H), 5.07 (m, 2H, Cp–H), 1.68 (s, 3H, C–Me), 1.55 (s, 3H, C–Me), 0.59 (s, 3H, Si–Me), 0.42 (s, 3H, Si–Me) ppm. IR (KBr): [ν_{CO}/cm^{-1}] 2025 s, 1956 s, 1938 s, 1925 s, 1914 s.

Photolysis of *trans*-2a with bromobenzene in C_6H_6.

A solution of *trans*-**2a** (39 mg, 0.05 mmol) and bromobenzene (79 mg, 0.50 mmol) in dry benzene (10 mL) in nitrogen flushed quartz tube was additionally degassed by bubbling nitrogen thru for 5 min. After irradiation for 3 h in the ice-water bath, the solvent was removed under the reduced pressure. The residue, which was dissolved in a minimum amount of CH_2Cl_2, was chromatographed in air on silica gel using petroleum ether as eluent. A colorless band was eluted and collected. Then, another colorless band was eluted with petroleum ether–CH_2Cl_2 (5:1). Then, a yellow band was eluted with petroleum ether–CH_2Cl_2 (3:1). Finally, another yellow was eluted with petroleum ether–CH_2Cl_2 (1:1). After vacuum removal of the solvents from the above three eluates, the last three residues were recrystallized from *n*-hexane/CH_2Cl_2 (1:1) at –10 °C. The first fraction afforded 8 mg of biphenyl as white solids. The second fraction contained unreacted *trans*-**2a** (2 mg, 5%). From the third fraction, 13 mg (28%) of red crystalline **4** was obtained. Anal. Calcd for $C_{19}H_{18}Br_2O_5Re_2Si_2$: C, 24.95; H, 1.98. Found: C, 24.72; H, 2.05. ^1H NMR (400 MHz, $CDCl_3$): δ 6.43 (m, 1H, C_5H_3), 5.62 (m, 2H, C_5H_3), 5.58 (m, 1H, C_5H_3), 5.35 (m, 2H, C_5H_3), 0.79 (s, 6H, $Si(CH_3)$), 0.43 (s, 6H, $Si(CH_3)$). ^{13}C NMR (100 MHz, $CDCl_3$): δ_c 193.5, 183.1 (*C*O), 112.0, 97.7, 97.5, 94.5, 92.2, 88.7 (Cp–*C*), 2.6, –0.7 (Me–*C*) ppm. IR (ν_{CO}, KBr): 2061 (s), 2025 (s), 1940 (s), 1908 (s) cm^{-1}. From the last fraction, 7 mg (13%) of red crystalline **5** was obtained. Anal. Calcd for $C_{18}H_{18}Br_4O_4Re_2Si_2$: C, 20.66; H, 1.73. Found: C, 20.75; H, 1.84. ^1H NMR (400 MHz, $CDCl_3$): δ 6.43 (t, J = 2.8 Hz, 2H, C_5H_3), 5.50 (t, J = 2.8 Hz, 4H, C_5H_3), 0.68 (s, 12H, $Si(CH_3)$). ^{13}C NMR (100 MHz, $CDCl_3$): δ_c 182.4 (*C*O), 109.1, 99.0, 95.0 (Cp–*C*), 1.8 (Me–*C*) ppm. IR (ν_{CO}, KBr): 2059 (s), 2026 (m), 2003 (s), 1997 (s) cm^{-1}.

Photolysis of *trans*-2b with bromobenzene in C_6H_6.

A solution of *trans*-**2b** (38 mg, 0.05 mmol) and bromobenzene (79 mg, 0.50 mmol) in dry benzene (10 mL) was irradiated for 3 h in the ice-water bath. Using the same method as in the reaction of *trans*-**2a** with bromobenzene, four bands were eluted from the silica gel column. The first fraction afforded 9 mg of biphenyl as white solids. The second fraction contained unreacted *trans*-**2a** (2 mg, 5%). From the third fraction, 14 mg (30%) of red crystalline **6** was obtained. Anal. Calcd for $C_{20}H_{18}Br_2O_5Re_2Si$: C, 26.73; H, 2.02. Found: C, 26.94; H, 1.89. ^1H NMR (400 MHz, $CDCl_3$): δ 6.18 (m, 1H, C_5H_3), 5.48 (m, 1H, C_5H_3), 5.45 (m, 1H, C_5H_3), 5.43 (m, 1H, C_5H_3), 5.39 (m, 1H, C_5H_3), 5.18 (m, 1H, C_5H_3), 2.04 (s, 3H, $C(CH_3)$), 1.47 (s, 3H, $C(CH_3)$), 0.82 (s, 3H, $Si(CH_3)$), 0.46 (s, 3H, $Si(CH_3)$). IR (ν_{CO}, KBr): 2060 (s), 2025 (s), 2015 (s), 1938 (s), 1906 (s) cm^{-1}. From the last fraction, 6 mg (12%) of red crystalline **7** was obtained. Anal. Calcd for $C_{19}H_{18}Br_4O_4Re_2Si$: C, 22.15; H, 1.76. Found: C, 22.63; H, 1.87. ^1H NMR (400 MHz, $CDCl_3$): δ6.09 (m, 2H, C_5H_3), 5.63 (m, 2H, C_5H_3), 5.37 (m, 2H, C_5H_3), 1.84 (s, 6H, $C(CH_3)$), 0.73 (s, 6H, $Si(CH_3)$). IR (ν_{CO}, KBr): 2056 (s), 2011 (m), 1997 (s), 1991 (s), 1983 (s) cm^{-1}.

Photolysis of *trans*-2a with chlorobenzene in C_6H_6.

A solution of *trans*-**2a** (39 mg, 0.05 mmol) and chlorobenzene (56 mg, 0.50 mmol) in dry benzene (10 mL) was irradiated for 6 h in the ice-water bath. Using the same method as in the reaction of *trans*-**2a** with bromobenzene, four bands were eluted from the silica gel column. The first fraction afforded 7 mg of biphenyl as white solids. The second fraction contained unreacted *trans*-**2a** (4 mg, 10%). From the third fraction, 11 mg (27%) of orange crystalline **8** was obtained. Anal. Calcd for $C_{19}H_{18}Cl_2O_5Re_2Si_2$: C, 27.63; H, 2.20. Found: C, 27.91; H, 2.09. ^{1}H NMR (400 MHz, $CDCl_3$): δ 6.62 (m, 1H, C_5H_3), 5.64 (m, 2H, C_5H_3), 5.58 (m, 1H, C_5H_3), 5.02 (m, 2H, C_5H_3), 0.75 (s, 6H, $Si(CH_3)$), 0.42 (s, 6H, $Si(CH_3)$). IR (ν_{CO}, KBr): 2072 (s), 2026 (s), 1943 (s), 1908 (s) cm^{-1}. From the last fraction, 4 mg (9%) of orange crystalline **9** was obtained. Anal. Calcd for $C_{18}H_{18}Cl_4O_4Re_2Si_2$: C, 24.89; H, 2.09. Found: C, 24.53; H, 1.90. ^{1}H NMR (400 MHz, $CDCl_3$): δ 6.57 (t, J = 2.8 Hz, 2H, C_5H_3), 5.24 (t, J = 2.8 Hz, 4H, C_5H_3), 0.63 (s, 12H, $Si(CH_3)$). IR (ν_{CO}, KBr): 2071 (s), 2016 (m), 2005 (s) cm^{-1}.

Photolysis of *trans*-2a with chlorobenzene in C_6H_6 (add in $CHBr_3$ after irradiation)

A solution of *trans*-**2a** (39 mg, 0.05 mmol) and chlorobenzene (56 mg, 0.50 mmol) in dry benzene (10 mL) was irradiated for 6 h in the ice-water bath, then the solution was added in 60 μL of $CHBr_3$ and kept at 50 °C for 0.5 h. Using the same method as in the reaction of *trans*-**2a** with bromobenzene, four bands were eluted from the silica gel column. The first fraction afforded 8 mg of biphenyl as white solids. The second fraction contained unreacted *trans*-**2a** (5 mg, 10%). From the third fraction, 6 mg (35%) of red crystalline **11** was obtained. Anal. Calcd for $C_{19}H_{18}BrClO_5Re_2Si_2$: C, 26.22; H, 2.08. Found: C, 26.39; H, 2.09. ^{1}H NMR (400 MHz, $CDCl_3$): δ 6.53 (m, 1H, C_5H_3), 5.63 (m, 2H, C_5H_3), 5.58 (m, 1H, C_5H_3), 5.18 (m, 2H, C_5H_3), 0.77 (s, 6H, $Si(CH_3)$), 0.43 (s, 6H, $Si(CH_3)$). IR (ν_{CO}, KBr): 2066 (s), 2020 (s), 1941 (s), 1907 (s) cm^{-1}. From the last fraction, trace amounts of orange crystalline **8** (less than 5%) was obtained.

Photolysis of *trans*-2a with iodobenzene in C_6H_6

A solution of *trans*-**2a** (39 mg, 0.05 mmol) and iodobenzene (102 mg, 0.50 mmol) in dry benzene (10 mL) was irradiated for 9 h in the ice-water bath. Using the same method as in the reaction of *trans*-**2a** with bromobenzene, three bands were eluted from the silica gel column. The first fraction afforded 4 mg of biphenyl as white solids. The second fraction contained unreacted *trans*-**2a** (10 mg, 25%). From the third fraction, 15 mg (30%) of red crystalline **10** was obtained. Anal. Calcd for $C_{19}H_{18}Cl_2O_5Re_2Si_2$: C, 22.62; H, 1.80. Found: C, 22.95; H, 2.02. ^{1}H NMR (400 MHz, CDCl$_3$): δ 6.05 (m, 1H, C_5H_3), 5.89 (m, 2H, C_5H_3), 5.58 (m, 3H, C_5H_3), 0.85 (s, 6H, Si(CH_3)), 0.47 (s, 6H, Si(CH_3)). IR (ν_{CO}, KBr): 2041 (s), 2021 (s), 2003 (s), 1930 (s), 1913 (s) cm^{-1}.

General Methods

A solution of *trans*-**2a** (39 mg, 0.05 mmol) and substituted chlorobenzene (0.50 mmol) in dry benzene (10 mL) in nitrogen flushed quartz tube was additionally degassed by bubbling nitrogen thru for 5 min. After irradiation for 2–6 h in the ice-water bath, the solvent was removed under the reduced pressure. The residue, which was dissolved in a minimum amount of CH_2Cl_2, was chromatographed in air on silica gel using petroleum ether–CH_2Cl_2 mixture as eluent. The first band (colorless) afforded the substituted biphenyl as white solids. The second band gave unreacted *trans*-**2a** (5-10%). The third band (yellow) gave the mono(rhenium dichloride) complex **4** (20–30%). The final band (yellow) afforded the di(rhenium dichloride) complex **5** (5–12%).

Photolysis of *trans*-2a with benzyl chloride in C_6H_6

A solution of *trans*-**2a** (39 mg, 0.05 mmol) and benzyl chloride (63 mg, 0.50 mmol) in dry benzene (10 mL) was irradiated for 5 h in the ice-water bath. Using the same method as in the reaction of *trans*-**2a** with bromobenzene, four bands were eluted from the silica gel column. The first fraction afforded 5 mg of diphenylmethane and bibenzyl mixture as the colorless oils (ratio is 3:5). The second fraction contained unreacted *trans*-**2a** (10 mg, 25%). From the third fraction, 6 mg (15%) of red crystalline **8** was obtained. From the last fraction, a trace amount of orange solid **9** (less than 5%) was obtained.

Photolysis of *trans*-2a with *n*-hexyl chloride in C_6H_6

A solution of *trans*-**2a** (39 mg, 0.05 mmol) and *n*-hexyl chloride (60 mg, 0.50 mmol) in dry benzene (10 mL) was irradiated for 8 h in the ice-water bath. Using the same method as in the reaction of *trans*-**2a** with bromobenzene, four bands were eluted from the silica gel column. The first fraction afforded a trace amount of *n*-dodecane as the colorless oil. The second fraction contained unreacted *trans*-**2a** (18 mg, 45%). From the third fraction, 6 mg (15%) of red crystalline **8** was obtained. From the last fraction, trace of orange solid **9** (less than 5%) was obtained.

Photolysis of *trans*-2a in C_6F_6

A solution of *trans*-**2a** (39 mg, 0.05 mmol) in C_6F_6 (10 mL) was irradiated for 5 h in the ice-water bath. Using the same method as described in the reaction of *cis*-**2a** with benzene, one dark yellow band were eluted from the silica gel column using petroleum ether–CH_2Cl_2 (1:5) as eluent. 15 mg (32%) of reddish brown crystalline **12** was obtained after recrystallization from *n*-hexane/CH_2Cl_2 (1:1) at –10 °C. Anal. Calcd for $C_{26}H_{18}F_6O_5Re_2Si_2$: C, 31.91; H, 1.93. Found: C, 32.15; H, 2.13. ^1H NMR (400 MHz, $CDCl_3$): δ 6.75 (m, 1H, C_5H_3), 6.50 (m, 1H, C_5H_3), 5.75 (m, 1H, C_5H_3), 5.72 (m, 1H, C_5H_3), 5.67 (m, 1H, C_5H_3), 5.61 (m, 1H, C_5H_3), 0.69 (s, 3H, $Si(CH_3)$), 0.65 (s, 3H, $Si(CH_3)$), 0.56 (s, 3H, $Si(CH_3)$), 0.48 (s, 3H, $Si(CH_3)$). ^{19}F NMR (400 MHz, $CDCl_3$): δ −162.67 (m, 2F, C_6F_5), −158.45 (m, 1F, C_6F_5), −131.93 (s, 1F, Re–*F*), −107.02 (m, 2F, C_6F_5). IR (ν_{CO}, KBr): 2041 (s), 2025 (s), 1969 (s), 1928 (s) cm^{-1}.

Crystallography

Single crystals of complexes *cis*-**2a**, *cis*-**2b**, *trans*-**2b**, **3b**, **6**, **7**, **8**, **11**, and **12** (CCDC reference numbers 1017441–1017449) suitable for X-ray diffraction were obtained by crystallization from *n*-hexane/CH_2Cl_2 (1:1). Data collection was performed on a Bruker SMART 1000, using graphite-monochromated Mo Kα radiation (ω–2θ scans, λ = 0.71073 Å). Semiempirical absorption corrections were applied for all complexes. The structures were solved by direct methods and refined by full-matrix least squares. All calculations were using the SHELXTL-97 program system. The crystal data and summary of X-ray data collection are presented in Tables 2-4.

Table 2. Crystal Data and Summary of X-ray Data Collection for *cis*-**2a**, *cis*-**2b**, and *trans*-**2b**.

	cis-**2a**	*cis*-**2b**	*trans*-**2b**
formula	$C_{20}H_{18}O_6Re_2Si_2$	$C_{21}H_{18}O_6Re_2Si$	$C_{21}H_{18}O_6Re_2Si$
fw	782.92	766.84	766.84
T (K)	296(2)	173(2)	173(2)
cryst syst	Triclinic	Monoclinic	Monoclinic
space group	P–1	P2(1)/c	P2(1)/n
a (Å)	7.173(2)	13.595(4)	10.1782(6)
b (Å)	9.475(3)	14.692(4)	16.396(1)
c (Å)	18.023(5)	11.089(3)	13.1427(8)
α (deg)	100.660(5)	90	90
β (deg)	98.400(4)	90.314(4)	95.524(1)
γ (deg)	102.954(5)	90	90
V (Å^3)	1150.4(6)	2215.0(10)	2183.1(2)
Z	2	4	4
D_{calc} (g·cm^{-3})	2.260	2.300	2.333
μ (mm^{-1})	10.650	11.008	11.169
F(000)	728	1424	1424
cryst size (mm)	0.18 × 0.17 × 0.10	0.14 × 0.10 × 0.08	0.15 × 0.14 × 0.13
max. 2θ (deg)	50.02	50.02	50.02
no. of reflns collected	5801	10872	10814
no. of indep reflns/R_{int}	3992/0.0224	3895/0.0382	3824/0.0441
no. of params	275	275	275
goodness-of-fit on F^2	1.086	1.042	1.031
R_1, wR_2 [$I > 2\sigma$(I)]	0.0599, 0.1608	0.0284, 0.0661	0.0280, 0.0684
R_1, wR_2 (all data)	0.0712, 0.1664	0.0328, 0.0678	0.0306, 0.0703
largest diff peak and hole (e Å^{-3})	3.461, −3.102	1.950, −2.148	1.194, −1.496

Table 3. Crystal Data and Summary of X-ray Data Collection for **3b**, **6**, and **7**.

	3b	**6**	**7**
formula	$C_{19}H_{14}O_6Re_2$	$C_{20}H_{18}Br_2O_5Re_2Si$	$C_{19}H_{18}Br_4O_4Re_2Si$
fw	710.70	898.65	1030.46
T (K)	296(2)	173(2)	173(2)
cryst syst	Triclinic	Monoclinic	Triclinic
space group	P–1	P2(1)/c	P–1
a (Å)	7.9128(7)	13.087(1)	9.7003(7)
b (Å)	11.502(1)	14.153(2)	14.541(1)
c (Å)	12.313(1)	13.589(2)	17.377(1)
α (deg)	63.258(1)	90	95.709(1)
β (deg)	73.735(1)	113.256(2)	91.872(1)
γ (deg)	74.924(1)	90	93.112(1)
V (Å^3)	948.91(14)	2312.5(4)	2433.4(3)
Z	2	4	4
D_{calc} (g·cm^{-3})	2.487	2.581	2.813
μ (mm^{-1})	12.777	13.996	16.581
F(000)	652	1648	1872
cryst size (mm)	0.15 × 0.14 × 0.13	0.18 × 0.14 × 0.13	0.18 × 0.17 × 0.15
max. 2θ (deg)	50.02	50.02	50.02
no. of reflns collected	4872	11592	12699
no. of indep reflns/R_{int}	3321/0.0125	4077/0.0528	8555/0.0350
no. of params	247	292	549
goodness-of-fit on F^2	1.048	1.164	1.014
R_1, wR_2 [$I > 2\sigma$(I)]	0.0196, 0.0490	0.0437, 0.0960	0.0349, 0.0813
R_1, wR_2 (all data)	0.0230, 0.0507	0.0483, 0.0980	0.0425, 0.0854
largest diff peak and hole (e Å^{-3})	1.292, –0.616	2.411, –2.554	1.716, –1.881

Table 4. Crystal Data and Summary of X-ray Data Collection for **8**, **11**, and **12**.

	8	**11**	**12**
formula	$C_{19}H_{18}Cl_2O_5Re_2Si_2$	$C_{19}H_{18}Br_{0.7}Cl_{1.3}O_5Re_2Si_2$	$C_{26}H_{20}Cl_2F_6O_5Re_2Si_2$
fw	825.81	856.94	1025.90
T (K)	173(2)	296(2)	173(2)
cryst syst	Monoclinic	Monoclinic	Triclinic
space group	P2(1)/c	P21/c	P−1
a (Å)	13.358(1)	13.548(3)	8.416(1)
b (Å)	14.035(1)	14.211(3)	12.443(2)
c (Å)	13.3278(9)	13.564(3)	16.137(3)
α (deg)	90	90	77.437(3)
β (deg)	112.967(1)	113.388(4)	78.046(3)
γ (deg)	90	90	78.139(3)
V (Å^3)	2300.7(3)	2396.9(9)	1590.8(5)
Z	4	4	2
D_{calc} (g·cm^{-3})	2.384	2.375	2.142
μ (mm^{-1})	10.878	11.530	7.916
F(000)	1536	1586	964
cryst size (mm)	0.18 × 0.17 × 0.15	0.28 × 0.12 × 0.11	0.18 × 0.17 × 0.15
max. 2θ (deg)	50.00	50.02	50.00
no. of reflns collected	13079	13693	8765
no. of indep reflns/R_{int}	4040/0.0293	4235/0.0699	5546/0.0334
no. of params	275	278	292
goodness-of-fit on F^2	1.017	1.036	1.058
R_1, wR_2 [$I > 2\sigma(I)$]	0.0188, 0.0387	0.0371, 0.0919	0.0525, 0.1250
R_1, wR_2 (all data)	0.0229, 0.0403	0.0466, 0.0979	0.0711, 0.1349
largest diff peak and hole (e Å^{-3})	0.804, −0.619	1.731, −1.866	3.270, −2.308

Acknowledgments

This work was financially supported by the National Natural Science Foundation of China (No. 21002069), the Natural Science Foundation of Tianjin (No. 14JCYBJC20300), and the Program for Innovative Research Team in University of Tianjin (TD12-5038).

Notes and references

1 A. H. Klahn, C. Leiva, K. Mossert, X. Zhang, *Polyhedron*, 1991, **10**, 1873–1876.

2 (a) D. Sutton, J.-M. Zhuang, *Organometallics*, 1991, **10**, 1516–1527; (b) A. Hosang, U. Englert, A. Lorenz, U. Ruppli, A. Salzer, *J. Organomet. Chem.*, 1999, **583**, 47–55.

3 (a) M.-G. Choi, R. J. Angelici, *J. Am. Chem. Soc.*, 1991, **113**, 5651–5657; (b) C. P. Casey, H. Sakaba, P. N. Hazin, D. R. Powell, *J. Am. Chem. Soc.*, 1991, **113**, 8165–8166; (c) C. P. Casey, A. D. Selmeczy, J. R. Nash, C. S. Yi, D. R. Powell, R. K. Hayashi, *J. Am. Chem. Soc.*, 1996, **118**, 6698–6706; (d) D. A. Valyaev, O. V. Semeikin, M. G. Peterleitner, Y. A. Borisov, V. N. Khrustalev, A. M. Mazhuga, E. V. Kremer, N. A. Ustynyuk, *J. Organomet. Chem.*, 2004, **689**, 3837–3846.

4 H. Chen, J. F. Hartwig, *Angew. Chem.*, *Int. Ed.*, 1999, **38**, 3391–3393.

5 (a) E. A. Cobar, R. Z. Khaliullin, R. G. Bergman, M. Head-Gordon, *Proc. Nat. Acad. Sci.*, 2007, **104**, 6963–6968; (b) D. J. Lawes, S. Geftakis, G. E. Ball, *J. Am. Chem. Soc.*, 2005, **127**, 4134–4135.

6 (a) D. J. Lawes, T. A. Darwish, T. Clark, J. B. Harper, G. E. Ball, *Angew. Chem.*, *Int. Ed.*, 2006, **45**, 4486–4490; (b) S. Geftakis, G. E. Ball, *J. Am. Chem. Soc.*, 1998, **120**, 9953–9954.

7 B. Kayser, M. J. Eichberg, K. P. C. Vollhardt, *Organometallics*, 2000, **19**, 2389–2392.

8 J. K. Hoyano, W. A. G. Graham, *Organometallics*, 1982, **1**, 783–787.

9 J. J. Carbó, O. Eisenstein, C. L. Higgitt, A. H. Klahn, F. Maseras, B. Oelckers, R. N. Perutz, *J. Chem. Soc.*, *Dalton. Trans.*, 2001, 1452–1461.

10 (a) F. Godoy, C. L. Higgitt, A. H. Klahn, B. Oelckers, S. Parsons, R. N. Perutz, *J. Chem. Soc.*, *Dalton. Trans.*, 1999, 2039–2047; (b) A. H. Klahn, M. H. Moore, R. N. Perutz, *J. Chem. Soc.*, *Chem. Commun.*, 1992, 1699–1701.

11 (a) A. Aballay, E. Clot, O. Eisenstein, M. T. Garland, F. Godoy, A. H. Klahn, J. C. Muñoz, B. Oelckers, *New J. Chem.*, 2005, **29**, 226–231; (b) A. Aballay, F. Godoy, G. E. Buono-Core, A. H. Klahn, B. Oelckers, M. T. Garland, J. C. Muñoz, *J. Organomet. Chem.*, 2003, **688**, 168–173; (c) A. H. Klahn, M. Carreño, F. Godoy, B. Oelckers, A. Pizarro, A. Toro, A. Reyes, *J. Cood. Chem.*, 2011, **54**, 379–388; (d) A. H. Klahn, A. Toro, B. Oelckers, G. E. Buono-Core, V. Manriquez, O. Wittke, *Organometallics*, 2000, **19**, 2580–2584; (e) Y.-X. He, D. Sutton, *J. Organomet. Chem.*, 1997, **538**, 49–56.

12 B. Zhu, X. Huang, X. Hao, Photochemical Reactions of (η^5-C_5R_5)Re$(CO)_3$ (R = Me or H) with Aryl Halides in Benzene: Stoichiometric Formation of Bipheny, Submitted for publication.

13 (a) M. Herberhold, M. Biersake, *J. Organomet. Chem.*, 1990, **381**, 379–389; (b) M. Herberhold, M. Biersake, T. E. Bitterwolf, A. L. Rheingold, *Z. NaturForsch. B: Chem. Soc.*, 1993, **48**, 161–170; (c) E. W. Abel, S. Moorehouse, *J. Organomet. Chem.*, 1971, **29**, 227–232.

14 F. W. B. Einstein, A. H. Klahn-Oliva, D. Sutton, K. G. Tyers, *Organometallics*, 1986, **5**, 53–59.

15 (a) R. B. King, R. H. Reimann, D. J. Darensbourg, *J. Organomet. Chem.*, 1975, **93**, C23–C25; (b) R. B. King, R. H. Reimann, *Inorg. Chem.*, 1976, **15**, 179–183.

16 (a) A. H. Klahn-Oliva, R. D. Singer, J. M. Aramini, D. Sutton, *Inorg. Chem.*, 1989, **28**, 4217–4221; (b) C. M. Nunn, A. H. Cowley, S. W. Lee, M. G. Richmond, *Inorg. Chem.*, 1990, **29**, 2105–2112.

17 Y.-R. Luo, *Handbook of Bond Dissociation Energies in Organic Compounds*; CRC Press: Florida, 2003.

18 A. H. Klahn, B. Oelckers, F. Godoy, M. T. Garland, A. Vega, R. N. Perutz, C. L. Higgitt, *J. Chem. Soc.*, *Dalton. Trans.*, 1998, 3079–3086.

19 (a) I. E. Nifant'ev, V. L. Yarnykh, M. V. Borzov, B. A. Mazurchik, V. I. Mstyslavsky, V. A. Roznyatovsky, Y. A. Ustynyuk, *Organometallics*, 1991, **10**,

3739–3745; (b) X.-F. Hou, P.-C. Zhang, S. Liu, H. Wang, Y.-J. Lin, G.-X. Jin, *J. Organomet. Chem.*, 2008, **693**, 1462–1468.

For table of contents use only:

Synthesis and Structures of Doubly-Bridged Dicyclopentadienyl Dinuclear Rhenium Complexes, and Their Photochemical Reactions with Aromatic Halides in Benzene

Bolin Zhu,* Xinwei Huang and Xiaoting Hao

Photolysis of doubly-bridged biscyclopentadienyl dirhenium carbonyl complexes *trans*-**2a**,**b** with aryl halides in benzene results in the formation of biphenyl stoichiometrically.